TITANITE U-PB AGE AND TRACE ELEMENT CHEMISTRY: TRACING COOLING AND ALTERATION IN THE SIERRA NEVADA BATHOLITH

HRUSKA, Grace, LACKEY, Jade Star and MCCARTY, Kyle R.,

Geology Department, Pomona College, 185 E. 6th St, Claremont, CA 91711

1. Motivation

Recent studies have proposed intriguing crystallization processes in relatively cold, sub-solidus conditions (Challener and Glazner, 2017; Ackerson et al. 2018) of granitoid rocks in the Sierra Nevada batholith (SNB). Such discoveries beg deeper investigation of the transition from magmatic to sub-solidus conditions in arc batholiths and hold potential for understanding their changing thermal state during the waxing and waning of magmatism. Understanding of this sub-solidus realm also bears on the fluid mediated formation of ore deposits and modulation of volatile fluxes (e.g., CO2). In this work, we have examined Pb-U systematics and trace element chemistry of both primary, euhedral titanite and co-existing, texturally late, anhedral titanite from ~30 rocks in the western, central, and eastern Sierra Nevada. In particular we sought to 1) evaluate relative Pb-U ages of titanite and zircon; 2) to probe the chemistry of secondary titanite as a recorder of the sub-solidus history of individual rocks as well as trends across the batholith.

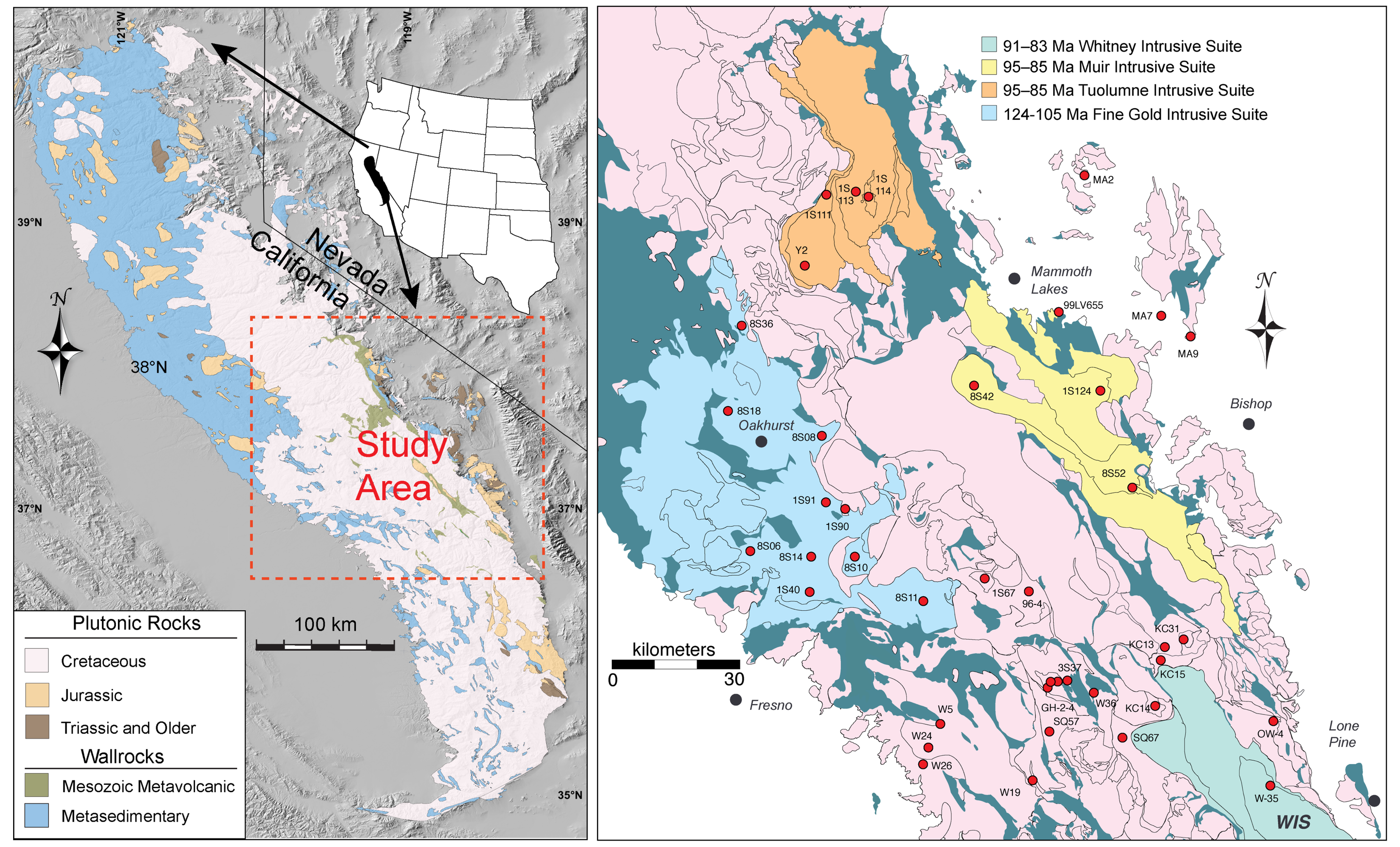

Figures 1&2: Simplified geologic map showing the regional extent of the SNB and relative ages of plutonic and wallrock units; study area shown with dashed red line (left). Map of study area intrusive suites and their respective age ranges, based on Lackey et al. (2008) and Coleman et al. (2004).

2. Sierra Nevada Titanite

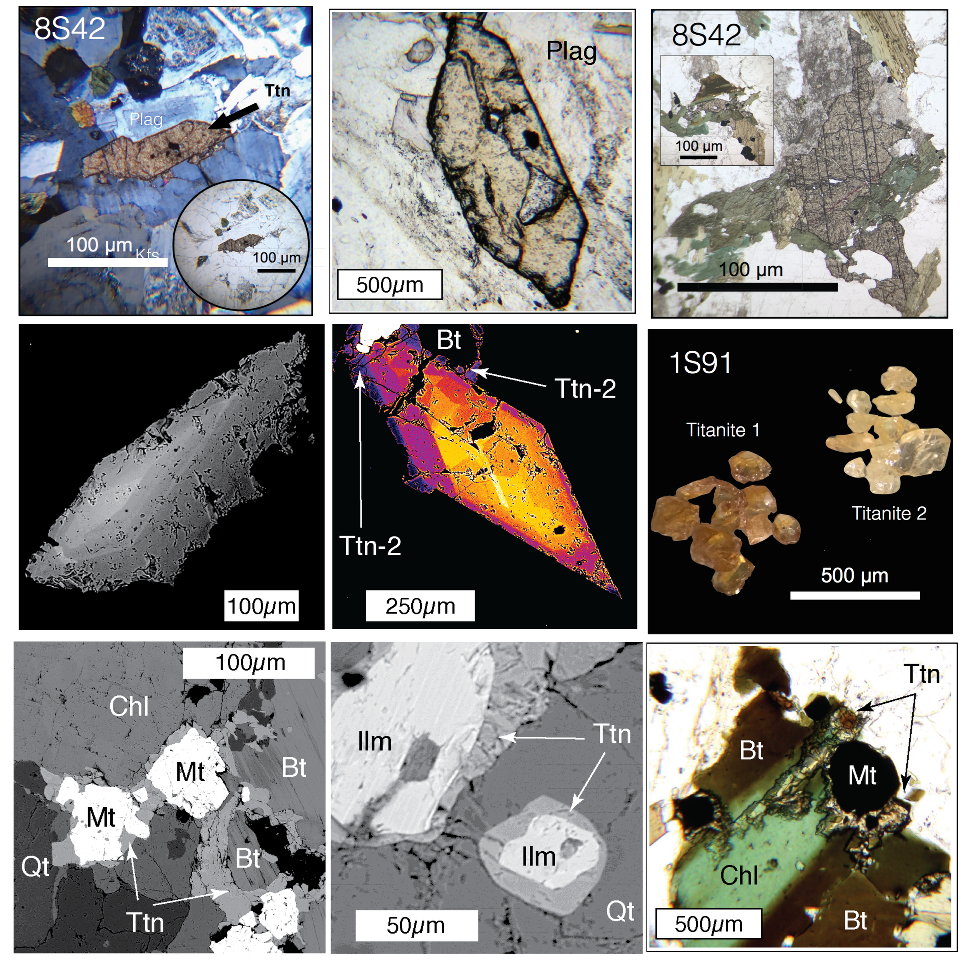

Figure 3: Textures of primary and secondary titanite. Primary titanite in top row shows euhedral look and is associated with feldspar, but often occurs in association with hornblende and/or biotite. Backscattered electron (BSE) image showing in second row, showing oscillatory zoning in primary and sector zoning in primary titanite crystals. Middle-right sample from 1S91 showing color difference between primary, brown-orange titanite and pale, secondary titanite from same rock. In third row, petrographic details of secondary titanite growth which typically is finer grained and forms coronas around oxides and where biotite is altered to chlorite.

Experiments: Primary and secondary titanite was hand picked from concentrates. Pb-U ages were measured at UC Santa Barbara after Kylander-Clark et al. (2013) and at Pomona College's Oxtoby Isotope Lab via laser ablation on an Agilent 8900 triple quadrupole mass spectrometer in He cell gas configuration. Titanite BLR and Y17 were employed as primary and secondary standards at UCSB. The Pomona lab employed MKED-1 and BLR-1 as primary standards for U-Pb and trace element concentrations, respectively. Previous titanium EMPA results of typical Sierra titanite were used as internal elemental standard values. NIST 612 was also analyzed as a validation standard for trace element determinations. Data was reduced using Iolite data reduction software.

3. Titanite Pb-U

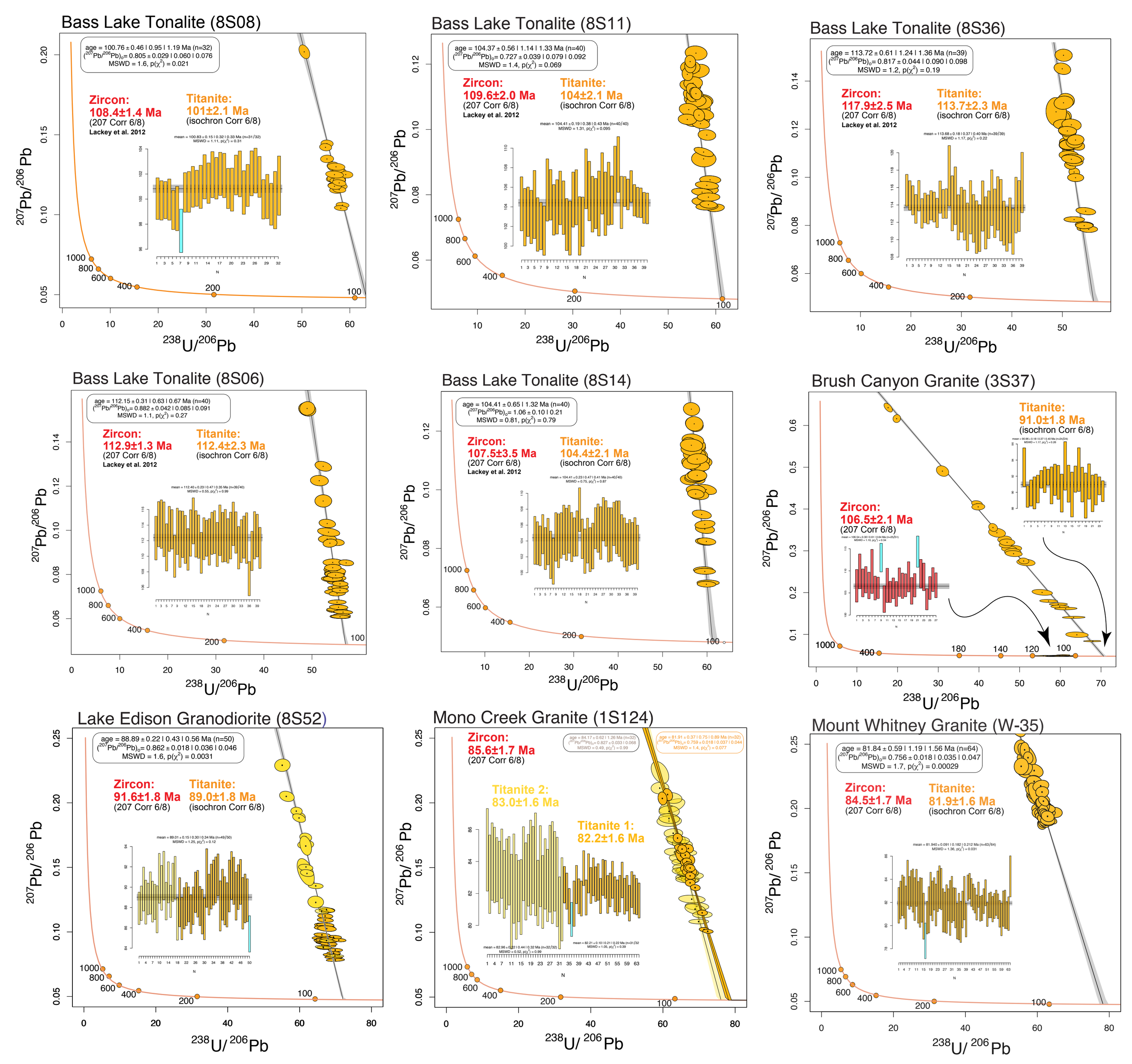

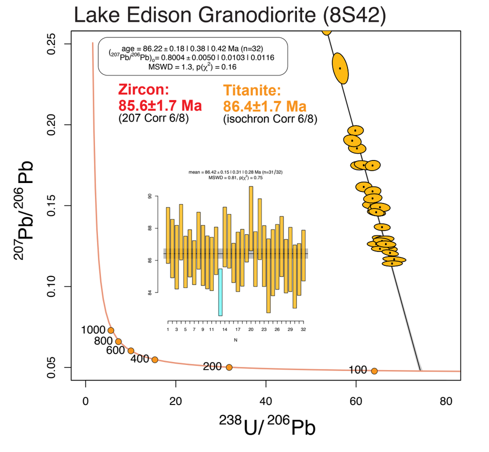

Figure 4: Tera-Wasserburg Concordia arrays defined by various SNB titanite (primary and secondary designated with different colors where analyzed). An additional 2% uncertainty is applied to the internal uncertainty of interpreted ^{207}Pb-corrected intercept titanite ages. Weighted Mean Pb-U plots of primary and secondary titanite samples display slightly different coordination in some cases. ^{207}Pb-corrected $^{206}Pb/^{238}U$ zircon ages from unpublished data and Lackey et al. (2012) shown for reference.

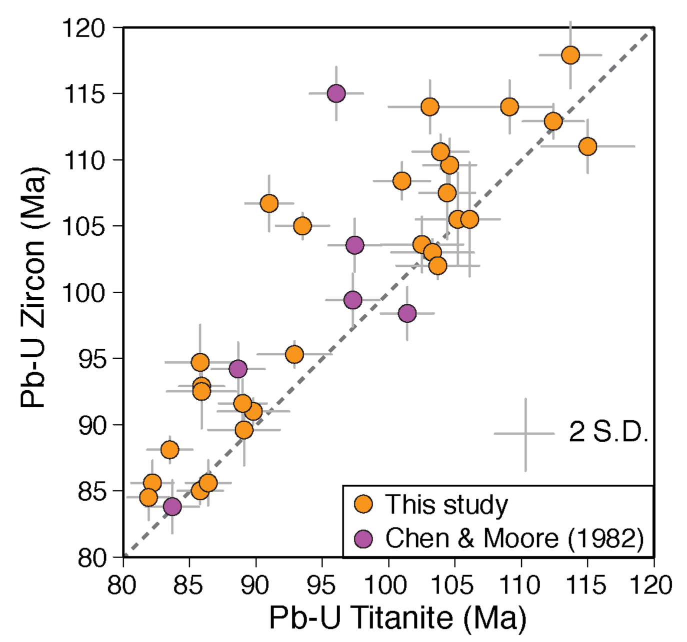

Figure 5: Correspondence of age for zircon and titanite shows variable offset to younger age of titanite compared to zircon, although often within error of the 1:1 dashed line which indicates analogous age. Some cases of titanite are up to 15 million years younger than zircon. Samples of Chen and Moore (1982) shown for reference.

4. Titanite Trace Elements

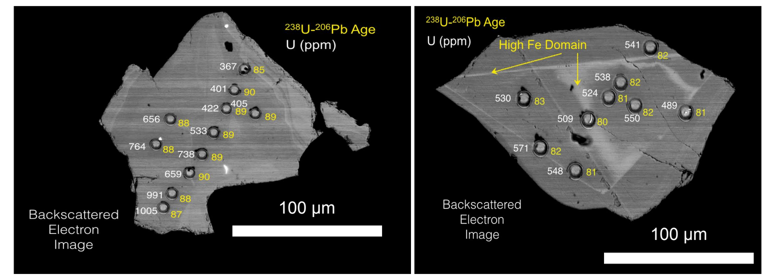

Figure 6: Backscattered electron (BSE) images of representative titanite samples in this study. Images show location of laser spots and values obtained via mass spectrometer. Rim-rim traverses across zoning and textural boundaries were performed.

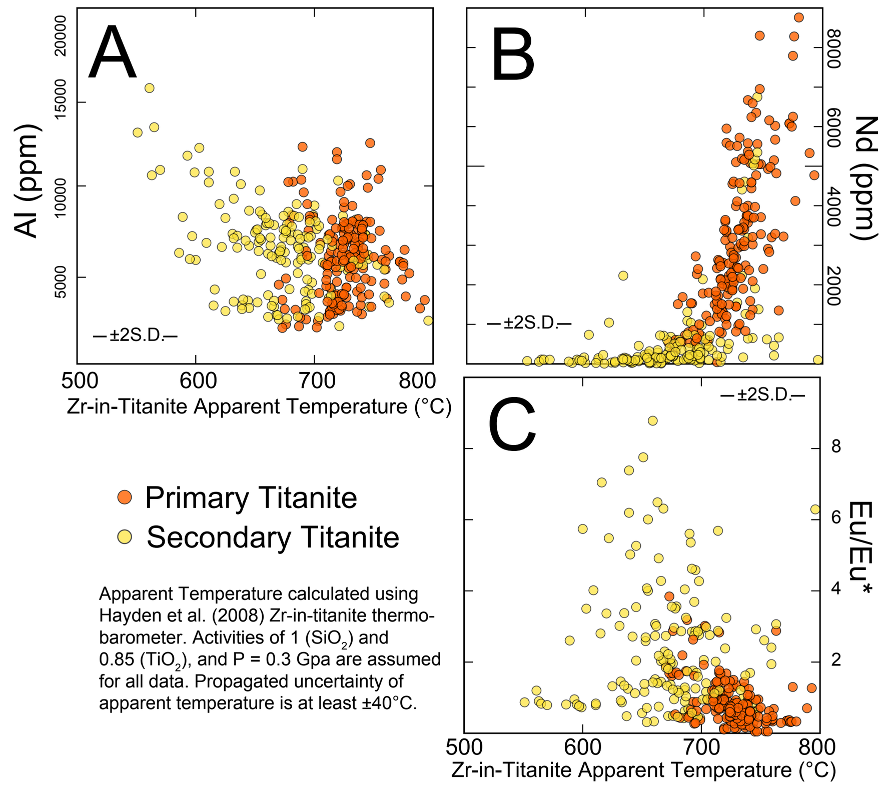

Figure 7: Zr-in-titanite apparent temperatures against selected major and trace element graphs of hand-picked primary and secondary titanite. (A) Aluminum (Al) concentrations in secondary titanite showing a subtle increase as apparent temperature decreases. (B) As seen in other REEs (Fig. 8), neodymium (Nd) concentrations tend to be higher in primary titanite versus secondary titanite. (C) Secondary titanite exhibiting a higher degree of Eu/Eu* magnitudes and variation compared to primary titanite.

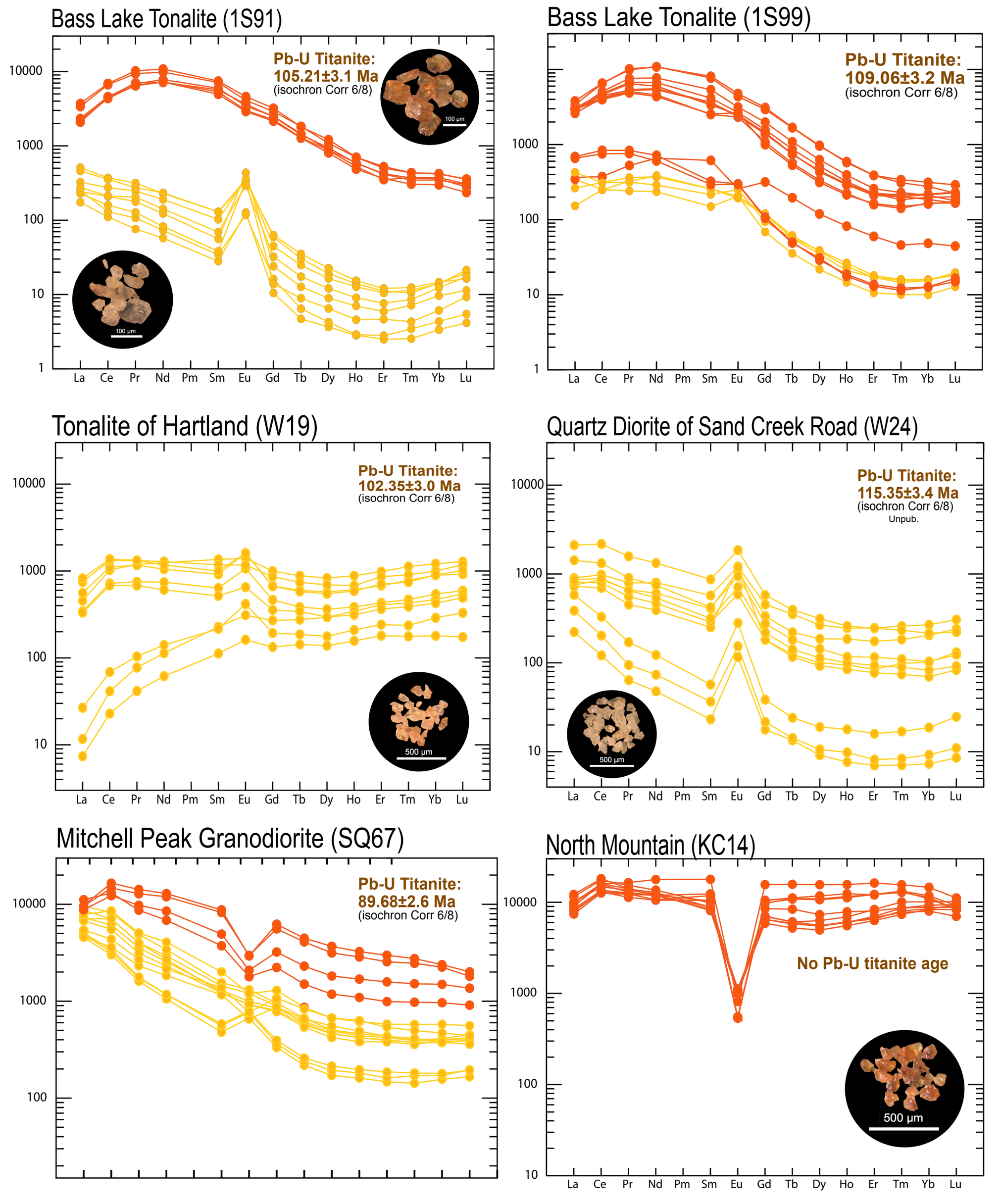

Figure 8: REE spider diagrams of SNB primary (red) and secondary (yellow) titanite, normalized to Chondrite from Sun-McDonough (1989) with corresponding ^{207}Pb-corrected 206/238 intercept ages.

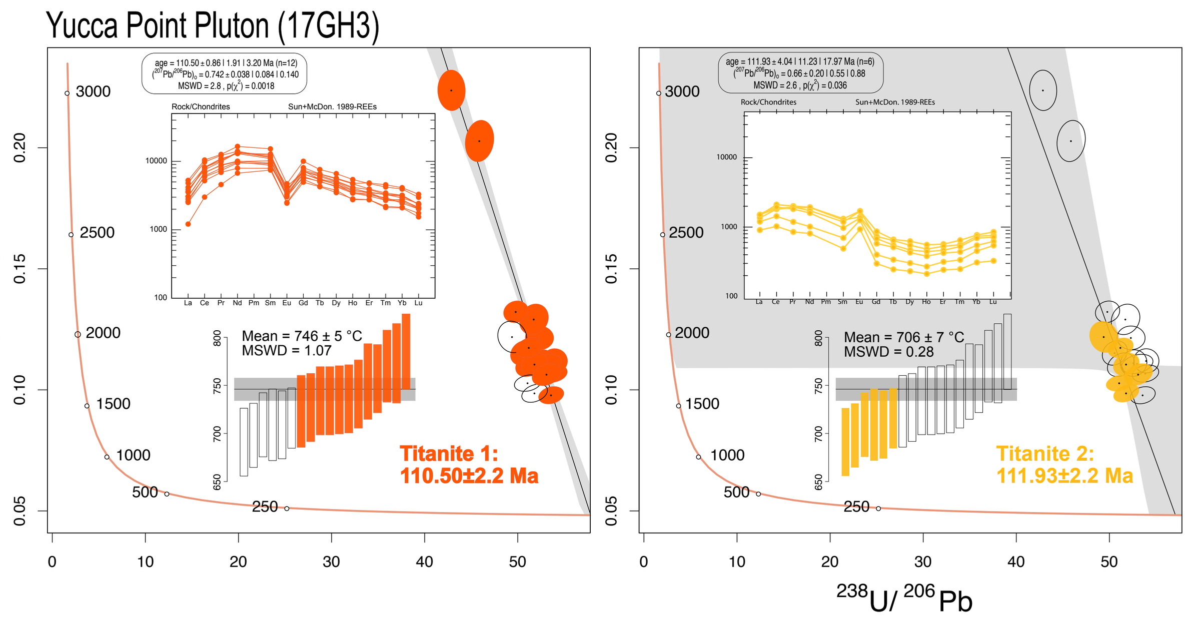

Figure 9: Titanite Tera-Wasserburg Concordia age diagram, REE plot, and histogram illustrating two different titanite populations from Sample 17GH3. Majority of the titanite within the samples analyzed are igneous (magmatic) and have trace element patterns consistent with magmatic growth. Secondary titanite has lower total REEs and positive Eu anomalies suggesting growth in equilibrium with deuteric fluids.

5. Oxygen Isotopes

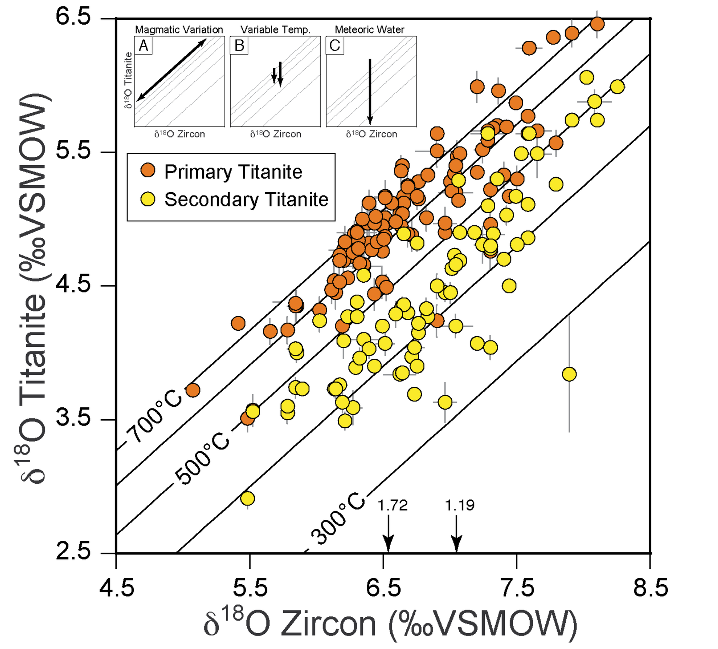

Figure 10: Variations of $\delta^{18}O$ in primary and secondary titanite with respect to $\delta^{18}O$ of zircon. Inset diagrams depict scenarios of expected $\delta^{18}O$ variation: (A) differing magmatic $\delta^{18}O$, (B) variable temperature of growth (or diffusive exchange), and (C) shifts expected from meteoric water exchange. Note the very low $\delta^{18}O$ values (< 2‰) of secondary titanite for two samples. Overall, a dearth of unusually low $\delta^{18}O$ values suggests that incursion of exogenous or meteoric water was limited, but deuteric fluid alteration, commonly indicated by retrogression of mafic minerals and feldspars, was likely widespread. Data compiled from Lackey et al. (2008) and Lackey (2005). Isotherms after King et al. (2001).

6. Models

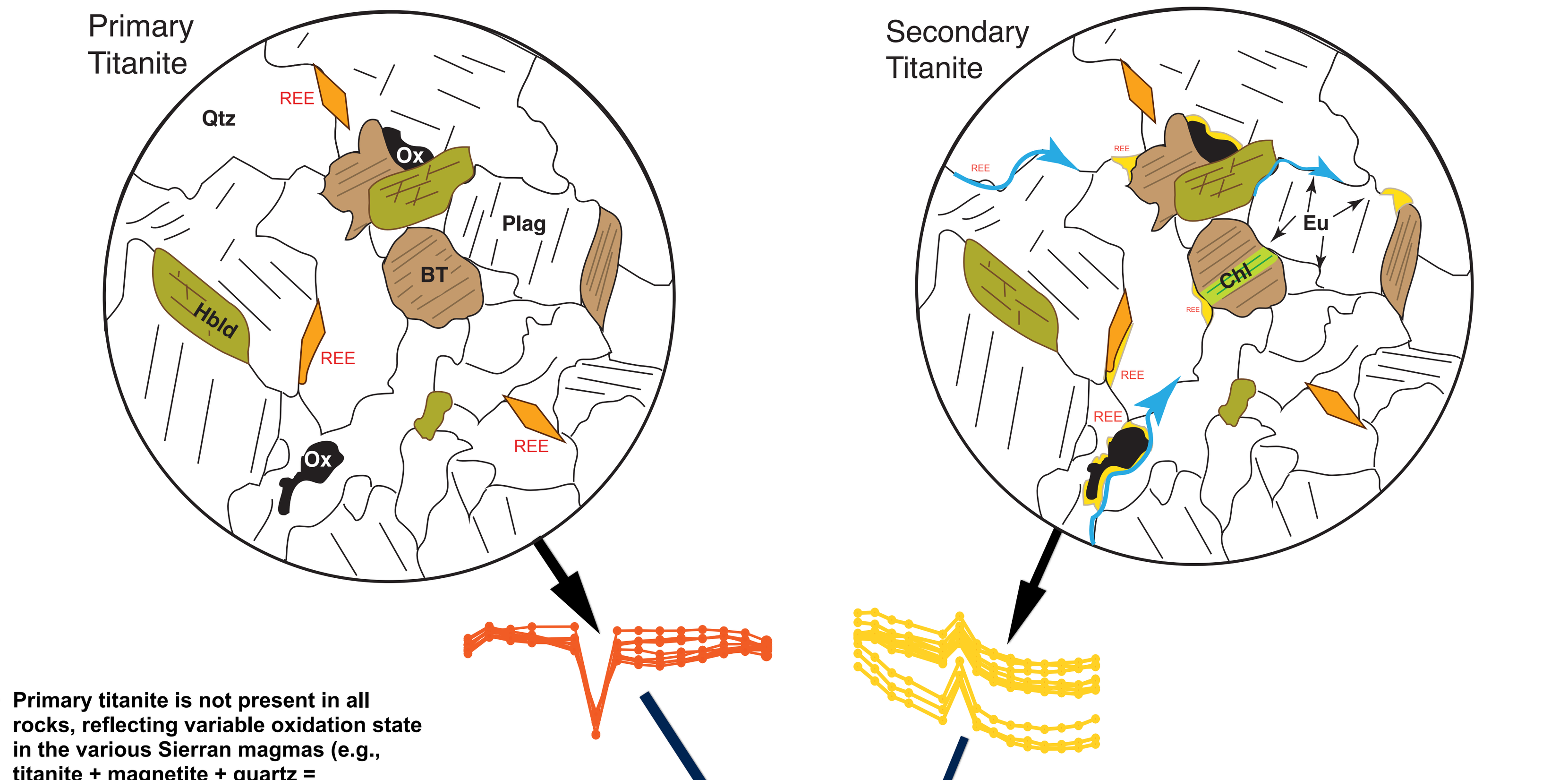

- Primary titanite is not present in all rocks, reflecting variable oxidation state in the various Sierran magmas (e.g., titanite + magnetite + quartz = hedenbergite + ilmenite + O_2; Wones (1989); and primary titanite may crystallize late during magmatic reaction of pyroxene to form hornblende, titanite, and ilmenite (Frost et al. 2001): Hedenbergite + ilmenite + H_2O = ferroactinolite + titanite +ulvöspinel.
- Stable by possible reactions
- REEs more uniformly budgeted

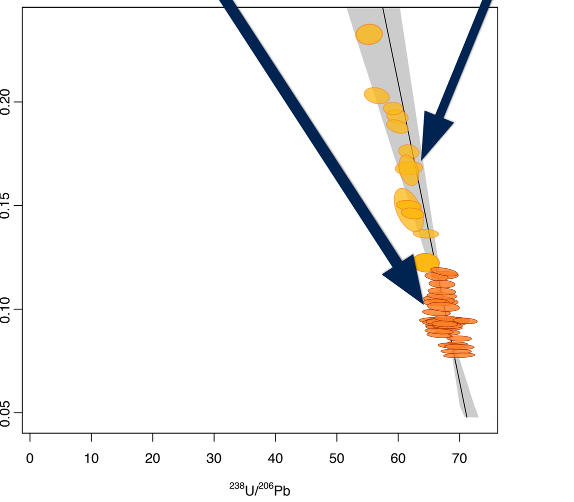

- Secondary titanite textures suggest a general pattern of increasingly oxidized systems and breakdown of pre-existing Ti-bearing phases in localized environments. REEs more heterogeneous as titanite competes with self
- Large positive Eu anomaly is suggesting more oxidized fluid
- Alternatively, liberation of Eu^{2+} with deuteric alteration of plagioclase may fix Eu concentrations and convert negative anomalies to positive anomalies.

7. Key Points

- Titanite ages often post-date U-Pb zircon, confirming patterns originally identified by Chen and Moore (1982); higher precision geo- and thermochronology will be needed to establish how cooling regime affects apparent age offsets.
- Secondary titanite shows distinct budget-limited depletion of REEs and greater variety in overall chemistry reflecting a mix of closed and open-system processes over a range of temperatures.
- Small, older plutons adjacent to large, late Cretaceous intrusive suites show lag of titanite U-Pb ages by up to 10 m.y., potentially a record of protracted growth, or re-crystallization (Schwartz et al. 2016), or potential thermal resetting.
- On a cautionary note, some late-stage titanite post-dates igneous crystallization ages by 10s of millions of years which warrants caution when interpreting detrital titanite U-Pb ages, in absence of REE patterns.
- Ongoing work is assessing intracrystalline patterns of Pb/U age and trace element concentration to establish if diffusional resetting or multiple growth episodes (e.g. Schwartz et al. 2016) explain marked age discrepancies in some titanite with igneous REE patterns.
- Overall, we note that Sierra Crest plutons have closer agreement of U-Pb age of zircon and titanite, suggesting that younger plutons saw a more rapid cooling, thus greater match of zircon and titanite U-Pb age. Western plutons, which may have seen titanite grow in response to changes of redox state in the sub-solidus, do not present a clear signal between diffusional Pb loss. We infer that growth of substantially younger (up to 10 million years) titanite was initiated as younger magmas caused re-equilibration of Fe-Ti oxide minerals with the younger deuteric fluids.

Cited Works

Ackerson, M.R., Mysen, B.O., Tailby, N.D., and Watson, E.B., 2018, Low-temperature crystallization of granites and the implications for crustal magmatism, Nature, v. 559, p. 94–97
Challener, S.C., and Glazner, A.F., 2017, Igneous or metamorphic? Hornblende phenocrysts as greenschist facies reaction cells in the Half Dome Granodiorite, California, American Mineralogist, v. 102, p. 436-444.
Chen, J.H., and Moore, J.G., 1982, Uranium-lead isotopic ages from the Sierra Nevada batholith, California: JGR Journal of Geophysical Research. B, v. 87, p. 4761-4784.
Coleman, D.S., Gray, W., and Glazner, A.F., 2004, Rethinking the emplacement and evolution of zoned plutons: geochronological evidence for incremental assembly of the Tuolumne ntrusive Suite, California: Geology, v. 32, p.433–436.
Hayden, L., Watson, E.B., and Wark, D.A., 2008, A thermobarometer for sphene (titanite): Contributions to Mineralogy and Petrology, v. 155, p. 529–540.
Frost, B.R., Chamberlain, K.R., and Schumacher, J.C., 2000, Sphene (titanite): phase relations and role as a geochronometer: Chemical Geology, p. 131–148.
King, E.M., Valley, J.W., Davis, D.W., and Kowallis, B.J., 2001, Empirical determination of oxygen isotope fractionation factors for titanite with respect to zircon and quartz: Geochimica et Cosmochimica Acta, v. 65, p. 3165-3175.
Kylander-Clark, A.R.C., Hacker, B.R., and Cottle, J.M., 2013, Laser-ablation split-stream ICP petrochronology: Chemical Geology, v. 345, p. 99–112.
Piccoli, P.M., and Candela, P.A., 1991, Zoning in titanite and f(O2) history, in Anonymous, ed., GSA Northeastern Section, 26th annual meeting; Southeastern Section, 40th annual meeting.: Abstracts with Programs - Geological Society of America: Boulder, CO, United States, Geological Society of America (GSA), p. 115.
Lackey, J.S., Cecil, M., Windham, C.J., Frazer, R.E., Bindeman, I.N., and Gehrels, G.E., 2012, The Fine Gold Intrusive Suite: The roles of basement terranes and magma source development in the Early Cretaceous Sierra Nevada batholith: Geosphere, v. 8, p. 292-313.
Lackey, J.S., Valley, J.W., Chen, J.H., and Stockli, D.F., 2008, Evolving magma systems, crustal recycling, and alteration in the central Sierra Nevada batholith: the oxygen isotope record: Journal of Petrology, v. 49, p. 1397–1426.
Schwartz, J.J., Stowell, H.H., Klepeis, K.A., Tulloch, A.J., Kylander-Clark, A.R.C., Hacker, B.R., and Coble, M.A., 2016, Thermochronology of extensional orogenic collapse in the deep crust of Zealandia: Geosphere, v. 12, no. 3, p. 647–677, doi:10.1130/GES01232.1.
Wones, D.R., 1989, Significance of the assemblage titanite+magnetite+quartz in granitic rocks: American Mineralogist, v. 74, p. 744-749.

Acknowledgements

We thank John Cottle and Andrew Kylander-Clark for assistance at the UCSB LASS lab and for follow-up advice with method developments in titanite and zircon LA-ICP-MS analyses in the Oxtoby Isotope lab at Pomona College. Josh Schwartz, Chloe Bonamici, and Mike Stearns have shared with us endless insight on titanite systematics. Samples analyzed here include those shared by Jim Chen from the Chen and Moore (1982) splits, Martha House, and Bill Hirt. This research was supported by a Pomona College faculty research grant. The Oxtoby Isotope Laboratory's LA-ICP-MS laboratory is funded by grant #5417 from the Gordon and Betty Moore Foundation.